Clinical Neurophysiology 121 (2010) 577–587

Contents lists available at ScienceDirect

Clinical Neurophysiology

journal homepage: www.elsevier.com/locate/clinph

Functional characterisation of sensory ERPs using probabilistic ICA: Effect of stimulus modality and stimulus location

M. Liang [a], A. Mouraux [b], V. Chan [a], C. Blakemore [a,c], G.D. Iannetti [a,d,*]

[a] Department of Physiology, Anatomy and Genetics, University of Oxford, UK
[b] Unité READ, Université catholique de Louvain, Belgium
[c] Department of Clinical Neurology, University of Oxford, UK
[d] Department of Neuroscience, Physiology and Pharmacology, University College London, UK

ARTICLE INFO

Article history:
Accepted 13 December 2009
Available online 27 January 2010

Keywords:
Event-related potentials (ERPs)
Auditory
Somatosensory
Visual
Probabilistic Independent Component Analysis (ICA)
Blind source separation

ABSTRACT

Objective: To decompose sensory event-related brain potentials (ERPs) into a set of independent components according to the modality and the spatial location of the eliciting sensory stimulus, and thus provide a quantitative analysis of their underlying components.

Methods: Auditory, somatosensory and visual ERPs were recorded from 124 electrodes in thirteen healthy participants. Probabilistic Independent Component Analysis (P-ICA) was used to decompose these sensory ERPs into a set of independent components according to the modality (auditory, somatosensory, visual or multimodal) and the spatial location (left or right side) of the eliciting stimulus.

Results: Middle-latency sensory ERPs were explained by a large contribution of multimodal neural activities, and a smaller contribution of unimodal neural activities. While a significant fraction of unimodal neural activities were dependent on the location of the eliciting stimulus, virtually all multimodal neural activities were not (i.e. their scalp distributions and time courses were not different when stimuli were presented on the left and right sides).

Conclusion: These findings show that P-ICA can be used to dissect effectively sensory ERPs into physiologically meaningful components, and indicate a new approach for exploring the effect of various experimental modulations of sensory ERPs.

Significance: This approach offers a better understanding of the functional significance of sensory ERPs.

1. Introduction

The recording of sensory event-related brain potentials (ERPs) is a widely used and non-invasive technique to sample directly the electrical activity of neurons and thereby gain knowledge about the neural basis of perception in humans (Luck, 2005). ERPs, which appear as transient changes in the ongoing electroencephalogram, time-locked to the onset of a sensory stimulus, are thought to result from synchronized changes of postsynaptic potentials, occurring in regularly oriented pyramidal neurons (Nunez and Srinivasan, 2006). Due to their high temporal resolution, ERPs allow unravelling the time course of cortical processes on a millisecond time-scale, and therefore complement the higher spatial resolution offered, for example, by functional magnetic resonance imaging (Iannetti et al., 2005).

One fundamental problem with interpreting ERPs is to quantify the contribution of different neural activities to the recorded signals. These neural activities are often referred to as *components*, each component being defined as the activity of a distinct neuroanatomical module contributing to a specific functional task (Luck, 2005).

There is a general agreement that short-latency ERPs (e.g. the N20 wave elicited by electrical stimulation of the median nerve, or the P100 wave elicited by visual stimulation) originate from primary sensory areas and predominantly reflect *unimodal* or *modality-specific* components (i.e. neural activities elicited by stimuli belonging to a specific sensory modality) (Regan, 1989). In contrast, longer-latency ERPs originate from multiple cortical areas and reflect a combination of both *unimodal* components and *multimodal* components (i.e. neural activities elicited by stimuli belonging to different sensory modalities) (Garcia-Larrea et al., 1995; Jutai et al., 1984; Naatanen and Picton, 1987).

Using a novel approach based on a Probabilistic Independent Component Analysis (P-ICA; Beckmann and Smith, 2004), we recently showed that it is possible to decompose ERPs elicited by a random sequence of auditory, visual and somatosensory stimuli

---

* Corresponding author. Address: Department of Neuroscience, Physiology and Pharmacology, University College London, Medical Sciences Building, Gower Street, London WC1E 6BT, UK. Tel.: +44 20 7679 3759.
E-mail address: g.iannetti@ucl.ac.uk (G.D. Iannetti).

1388-2457/$36.00 © 2009 International Federation of Clinical Neurophysiology. Published by Elsevier Ireland Ltd. All rights reserved.
doi:10.1016/j.clinph.2009.12.012

into their *unimodal* and *multimodal* components (Mouraux and Iannetti, 2009). Middle-latency (100–400 ms) auditory[1], visual and somatosensory potentials, which represented the largest part of the recorded ERPs, were explained by a predominant contribution of *multimodal* components, possibly related to mechanisms of stimulus-triggered arousal or attentional orientation, and by a less prominent contribution of *unimodal* components, restricted to the early part of the ERP response.

The finding that P-ICA can be used to separate effectively sensory ERPs into their respective *unimodal* and *multimodal* components opens new perspectives to dissect further sensory ERPs and thus understand better their functional significance. Here, using the same approach, we analysed ERPs elicited by auditory, somatosensory and visual stimuli applied to or near the left and right hand dorsum, with the aim of addressing two questions.

First, is the scalp distribution of *multimodal* neural activities determined by the spatial location of the stimulus? Experimental evidence indicates the existence of cortical responses that are influenced by the spatial location of the eliciting stimulus, independently of its sensory modality. For example, using BOLD-fMRI in humans, it has been shown that both auditory and visual stimuli presented on one side of the body elicit greater activity in the contralateral than ipsilateral intra-parietal sulcus (Macaluso and Driver, 2001). Furthermore, using single-cell recordings in macaque monkeys, neurons responding to both tactile and visual stimuli applied to the contralateral side of the body have been identified in the putamen, the parietal cortex and the inferior premotor cortex (Avillac et al., 2007; Duhamel et al., 1998; Fogassi et al., 1996; Graziano and Gross, 1993; Graziano and Gross, 1995). In addition, neurons involved in the multisensory integration of visual, somatosensory and proprioceptive information, and whose activity is dependent on the spatial location of body segments have been described in the premotor cortex and the posterior parietal cortex (Graziano, 1999; Graziano et al., 2000; Maravita et al., 2003). These results suggest that the scalp distribution of at least a fraction of the *multimodal* neural activities underlying ERPs could be dependent on the spatial location of the stimulus.

Second, what is the relative contribution of *location-dependent* and *location-independent unimodal* neural activities? It is well known that the topographic arrangement of neurons in primary somatosensory and visual cortices convey information about the location of the stimulus on the body or in the external world, i.e., neurons in different cortical regions respond to stimuli presented in different locations of the receptive surface. Therefore, one would expect neural activities elicited in primary sensory cortices to encode some information about the spatial location of the stimulus. Furthermore, like early-latency ERPs, middle-latency ERPs are also determined by the spatial location of the stimulus, and often display a scalp distribution with a maximum contralateral to the stimulated side (Ikeda et al., 1998; Srebro, 1985, 1987; Treede et al., 1988; Treede and Kunde, 1995). However, are all *unimodal* neural activities *location-dependent*, or are there also *location-independent unimodal* components?

In order to address these two questions, we applied P-ICA (Beckmann and Smith, 2004; Makeig et al., 1997) to 124-channel scalp ERPs. By comparing the ERPs elicited by a random sequence of stimuli belonging to three different sensory modalities (auditory, somatosensory and visual) and delivered at two different locations (left or right hand), we were able to quantify and characterise, at single-subject level, the contribution of neural activities depending on the modality and the spatial location of the eliciting stimulus to the ERP response.

2. Methods

2.1. Participants

Thirteen healthy volunteers (2 females; aged 25 ± 6 years old; 1 left handed) participated in the study. Before the electrophysiological recording, participants were familiarized with the experimental setup and the psychophysical rating task. They were also exposed to a small number of test stimuli (5–10 stimuli for each stimulus type). All experimental procedures were approved by the Oxfordshire Research Ethics Committee. Written informed consent was obtained from all participants.

2.2. Experimental design

The experiment took place in a dim, quiet and temperature-controlled room. Participants were seated in a comfortable armchair placed in front of a desk. They were told to relax, minimize eye blinks, and keep their gaze fixed on a white cross (3×3 cm) placed centrally in front of them, at an eye-distance of approximately 40 cm. Brief stimuli belonging to three different sensory modalities (auditory, somatosensory and visual) were intermixed and randomly delivered to or near the dorsum of the left or of the right hand (Fig. 1), to ensure that differences in the recorded responses were not related to differences in spatial attention (an experimental factor that has been shown to influence the magnitude and scalp topography of ERPs; Legrain et al., 2002; Schlereth et al., 2003). Only one stimulus belonging to one sensory modality was delivered on each trial. Thus, multimodal (i.e. concomitant) stimuli were never delivered, and the terms *Unimodal* and *Multimodal* used in the text only refer to the ERP components. The stimuli were presented in four successive blocks. The number of stimuli in each block ranged from 55 to 65. In total, 80 stimuli were presented for each sensory modality (40 on the left side and 40 on the right side)[2]. The inter-stimulus interval varied randomly between 5 and 10 s (rectangular distribution). Each block was separated by a 3–5 min break. To ensure that vigilance was maintained across time, and that each type of sensory stimulus was equally relevant to the task, participants were instructed to report the total number of perceived stimuli at the end of each of the four blocks. At the end of the experiment, participants were asked to rate the saliency of each type of stimulus using a numerical rating scale ranging from 0 (not salient) to 10 (extremely salient). Stimulus saliency was explained to the participant as "the ability of the stimulus to capture attention". Therefore, the rating was expected to integrate several factors such as stimulus intensity, frequency of appearance, novelty and its potential relevance to behaviour (Mouraux and Iannetti, 2009). As shown by Kayser et al. (2005), human ratings of saliency correlate well with predicted models of saliency.

2.3. Stimuli

The hands of the participants were placed at an eye-distance of approximately 45 cm, 25° left or right from the midline, 30° below eye-level. *Auditory stimuli* were brief 800 Hz tones (50 ms duration; 5 ms rise and fall times) presented at a comfortable listening level (~85 dB SPL), and delivered through a speaker (VE100AO, Audax, France) located immediately behind the left and right hands (~55 cm from the subject and ~22 cm from the midline). *Somatosensory stimuli* were constant current square-wave electrical pulses (1 ms duration; DS7A, Digitimer Ltd, UK) delivered through a pair of skin electrodes (1 cm inter-electrode distance) placed at the left

---

[1] Note that in auditory ERP studies, AEPs with latencies ranging between 10 and 50 ms are sometimes labelled as middle-latency AEPs.

[2] Note that the relatively small number of trials may have limited the ability to resolve short-latency sensory ERPs, therefore we focused our analysis on middle-latency sensory ERPs.

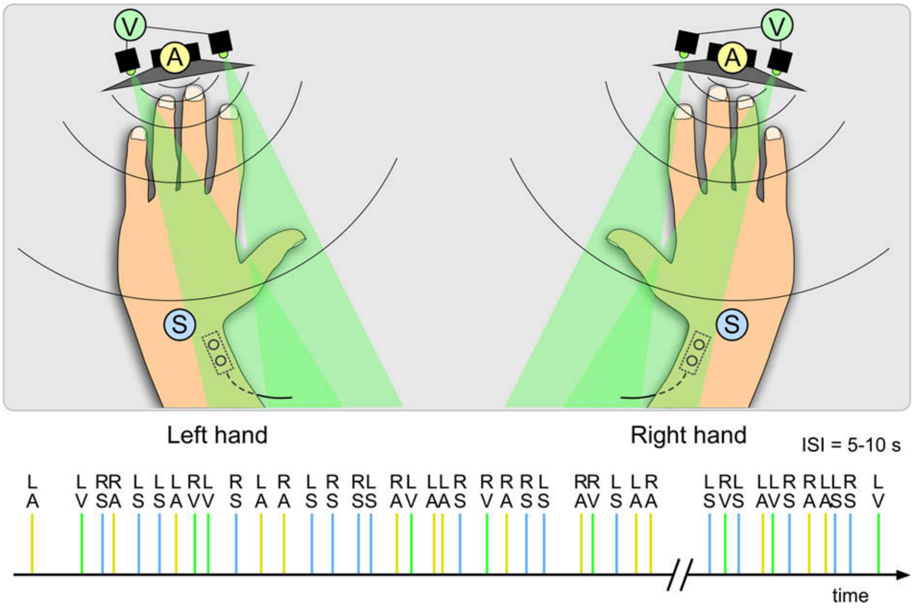

Fig. 1. Sensory stimulation. 124-Channel event-related potentials (ERPs) were elicited by a random sequence of auditory (A), somatosensory (S) and visual (V) stimuli. All stimuli were delivered to or near the hand dorsum, either on the left (L) or on the right (R) side, using an inter-stimulus interval of 5–10 s. *Auditory stimuli* (yellow) were brief 800 Hz tones presented at a comfortable listening level (~85 dB SPL) through a speaker located immediately behind the left and right hands. *Somatosensory stimuli* (light blue) were brief electrical pulses (1 ms duration) delivered though surface electrodes (represented in the figure with dashed lines) placed over the median nerve. For each participant, the intensity of the somatosensory stimulus was adjusted just above the threshold to elicit a small twitch of the thumb. *Visual stimuli* (light green) were brief flashes (50 ms duration) delivered through two green light-emitting diodes (11.6 cd) mounted on the top of the two speakers. For each type of stimulus, the intensity of the stimulation was adjusted until the participants reported similar intensities of perception for left- and right-side stimulation. (For interpretation of colour mentioned in this figure legend the reader is referred to the web version of the article.)

and the right wrists, over the median nerve. *Visual stimuli* were brief flashes (50 ms duration) delivered through two green light-emitting diodes (11.6 cd, 15° viewing angle) mounted on the top of the two speakers. For each participant, the intensity of the electric somatosensory stimulus was set slightly above the threshold to elicit a small twitch of the thumb. For each type of stimulus, the position and orientation of the stimulators were adjusted until the participants reported similar intensities of perception for left and right stimulation.

2.4. Control experiment

Since the auditory stimuli were delivered through speakers and thus perceived binaurally[3], we examined whether participants were able to discriminate correctly the side of sensory stimulation. In this control experiment, conducted on four of the subjects that participated in the ERP experiment, auditory, visual and somatosensory stimuli were presented using the same experimental setup. After each trial, participants were instructed to report whether the stimulus was presented on the right side or on the left side.

2.5. EEG recordings

The EEG was recorded using 124 electrodes placed on the scalp according to the International 10-5 system, using the nose as reference[4]. Ocular movements and eye blinks were recorded using two surface electrodes, one placed over the right lower eyelid, the other placed approximately 1 cm lateral to the lateral corner of the right orbit. The electrocardiogram was recorded using two surface electrodes placed on the volar surface of the left and right forearms. Signals were amplified and digitized using a sampling rate of 512 Hz (SD128, Micromed, Italy). Signal pre-processing was conducted using Letswave (http://amouraux.webnode.com/letswave, Mouraux and Iannetti, 2008). EEG signals were segmented into separate 1.5 s epochs (ranging from −0.5 to +1 s relative to stimulus onset), baseline corrected (baseline interval ranging from −0.5 to 0 s) and band-pass filtered (1–30 Hz). Artifacts produced by eye blinks or eye movements were subtracted using a validated method based on ICA (Jung et al., 2000). In addition, epochs with amplitude values exceeding ±100 μV (i.e., epochs likely to be contaminated by an artifact) were rejected. These epochs constituted 1 ± 1% of the total number of epochs. Remaining epochs were then averaged for each stimulus type, resulting in six average ERP waveforms (auditory left, auditory right, somatosensory left, somatosensory right, visual left and visual right) for each participant.

2.6. Blind source separation using P-ICA

For each participant, a blind source separation of ERPs was performed using an Independent Component Analysis (ICA; Makeig et al., 1997) constrained to an effective estimate of the intrinsic dimensionality of the original data (P-ICA; Beckmann and Smith, 2004; Mouraux and Iannetti, 2009).

When applied to multi-channel EEG recordings, ICA separates the signals recorded on the scalp into a linear combination of independent components (ICs), each having a fixed scalp topography and a maximally independent time course. When ICA is unconstrained, the total number of ICs equals the total number of recording electrodes. If the number of ICs differs greatly from the actual number of independent sources contributing to the signal, this may constitute a critical problem (Beckmann and Smith, 2004).

---

[3] The need of matching the location of the different stimuli to avoid differences related to spatial attention justified the choice of delivering the auditory stimuli using loudspeakers placed in the vicinity of the left and right hands.

[4] Note that we chose to use the nose as reference, and not an average reference, in order to avoid distorting and reducing widely-spread brain responses originating from deep cortical structures such as the anterior cingulate cortex (a potential area which is involved in multimodal sensory processing) and the operculo-insular cortex (a potential area which is involved in somatosensory and multimodal processing). A comparison between the results obtained using nose reference and average reference is shown in Supplementary Fig. S1.

Indeed, if the number of ICs is much larger than the number of sources, ICs containing spurious activity will appear because of overfitting. On the contrary, if the number of ICs is much smaller than the number of sources, valuable information will be lost because of underfitting. The problem of overfitting could be particularly important when unconstrained ICA is applied to averaged ERP waveforms. Indeed, because the averaging procedure cancels out sources of activity unrelated to the stimulus (e.g. ongoing EEG activity, muscular activity and noise), the number of independent sources present in the average waveform may be far smaller than the number of independent sources present in the original EEG signal. This fundamental limitation can be addressed using P-ICA, a method that constrains the number of estimated ICs to an effective estimate of the number of independent sources contributing to the original data, originally developed for the analysis of fMRI signals (Beckmann and Smith, 2004). It is worth noting that the statistical independence between each IC does not imply that each IC necessarily reflects the electrocortical activity generated by a single compact population of neurons (i.e. the activity of a single source). Indeed, if two or more spatially-distinct populations of neurons are activated synchronously, their activity will not separate into distinct ICs. Nevertheless, the obtained IC will still reflect a functionally-independent "network" of multiple sources.

For each subject, auditory, somatosensory and visual ERP waveforms following left and right stimulation were concatenated into a single waveform (six average waveforms × 1.5 s × 512 Hz = 4608 time points). P-ICA was then performed on this concatenated waveform in two steps. (1) An objective estimate of the number of independent sources contributing to the concatenated waveform was obtained using a method based on maximum likelihoods, and operating on the eigenvalues of a Principal Component Analysis (Rajan and Rayner, 1997). (2) ICA was performed on the concatenated waveform, constrained to the estimated number of dimensions, using runica (Delorme and Makeig, 2004; Makeig et al., 1997), an automated form of the extended infomax ICA algorithm (Bell and Sejnowski, 1995).

2.7. IC classification

We assumed that the ERPs elicited by each of the six stimulus types resulted from a linear mixture of *Unimodal* and *Multimodal* components, either *Location-dependent* or *Location-independent*, each component having a fixed scalp topography. *Unimodal* components are defined as components reflecting neural activity contributing only to the ERPs elicited by stimuli belonging to a specific sensory modality, while *Multimodal* components are defined as components reflecting neural activity contributing to the ERPs elicited by stimuli belonging to any sensory modality. *Location-dependent* components are defined as components reflecting neural activity contributing only to the ERPs elicited by stimuli delivered to one side of the body (i.e., contributing only to the ERPs elicited by left-side stimulation or contributing only to the ERPs elicited by right-side stimulation), while *Location-independent* components are defined as components reflecting neural activity contributing to the ERPs elicited by stimuli delivered to the right side of the body *as well as* to the ERPs elicited by stimuli delivered to the left side of the body (i.e., regardless of stimulus location).

According to these definitions, *Multimodal Location-independent* components would contribute to the ERPs elicited by all types of stimuli (i.e. regardless of sensory modality and stimulus location), while *Multimodal Location-dependent* components would contribute to the ERPs elicited by stimuli delivered to either the left or the right side, regardless of sensory modality. Similarly, *Unimodal Location-independent* components would contribute only to the ERPs elicited by stimuli belonging to a specific sensory modality, but regardless of stimulus location (e.g. *Auditory-specific Location-independent* neural activity would contribute to the left and the right AEP segments but not to the SEP or VEP segments), while *Unimodal Location-dependent* components (left or right) would contribute only to the ERPs elicited by stimuli belonging to a specific sensory modality and delivered to either the left or the right side (e.g. *right somatosensory-specific* neural activity would contribute only to the SEP elicited by right hand stimulation). Importantly, the classification of ICs as *Location-dependent* or *Location-independent* was thus not based on whether their scalp expression appeared bilateral or unilateral, but on whether or not they contributed uniquely to the response elicited by stimuli delivered to one side of the body.

The classification algorithm is outlined in Fig. 2. For each subject, ICs were first classified into the following three main categories: *Unimodal*, *Multimodal* and *Noise*. *Unimodal* ICs and *Multimodal* ICs were then further divided into two groups (*Location-dependent* and *Location-independent*), according to whether they contributed to the ERPs elicited by stimuli presented either on one side or on both sides.

In order to perform an objective classification of each IC into these five categories, it was necessary to estimate the relative contribution of each IC to the ERP elicited by each of the six stimulus types. For this purpose, the time course of the power of each IC (μV^2) was expressed as the standard deviation from the mean (Z scores) of the concatenated pre-stimulus intervals of all six average waveforms (−0.5 to 0 s). The Z scores were then averaged within the time interval of 0 to +0.5 s following the onset of each stimulus to estimate the relative contribution of each IC to each of the six ERP waveforms, thus yielding six average Z scores for each IC (Z_{AL}, Z_{AR}, Z_{SL}, Z_{SR}, Z_{VL}, Z_{VR}). Each IC was thus classified into one of the following five categories (Fig. 2):

2.7.1. Noise

If all six average Z scores (Z_{AL}, Z_{AR}, Z_{SL}, Z_{SR}, Z_{VL}, Z_{VR}) were smaller than 1.5, the IC was classified as noise.

2.7.2. Unimodal vs. Multimodal

Z scores of the ERPs following left and right stimulation were averaged within each modality (e.g. Z_{AL} and Z_{AR}), resulting in one Z score for each sensory modality (e.g. Z_A). If the ratios between the Z score of a specific modality and the Z scores of the other two modalities were both greater than 3.5 (e.g. $Z_A/Z_V > 3.5$ and $Z_A/Z_S > 3.5$), the IC was classified as *Unimodal*. Otherwise, it was classified as *Multimodal*.

2.7.3. Unimodal Location-dependent vs. Unimodal Location-independent

If an IC was classified as *Unimodal*, the Z scores of the ERPs elicited by left and right-side stimuli belonging to this modality were compared to determine whether the IC was *Location-dependent* or *Location-independent*. If the ratio between the two Z scores was greater than 3.5 (e.g. $Z_{AL}/Z_{AR} > 3.5$), the IC was classified as *Unimodal Location-dependent*. Otherwise, it was classified as *Unimodal Location-independent*.

2.7.4. Multimodal Location-dependent vs. Multimodal Location-independent

If an IC was classified as *Multimodal*, the Z scores of the ERPs elicited by left and right-side stimuli were compared for all three sensory modalities. If the ratio between the two Z scores was greater than 3.5 for at least two modalities (e.g. $Z_{AL}/Z_{AR} > 3.5$ and $Z_{SL}/Z_{SR} > 3.5$), the IC was classified as *Multimodal Location-dependent*. Otherwise, it was classified as *Multimodal Location-independent*.

It is important to highlight that the obtained classification was not critically dependent on the arbitrarily defined thresholds of 1.5 used to classify the ICs as non-noise-related and 3.5 used to classify

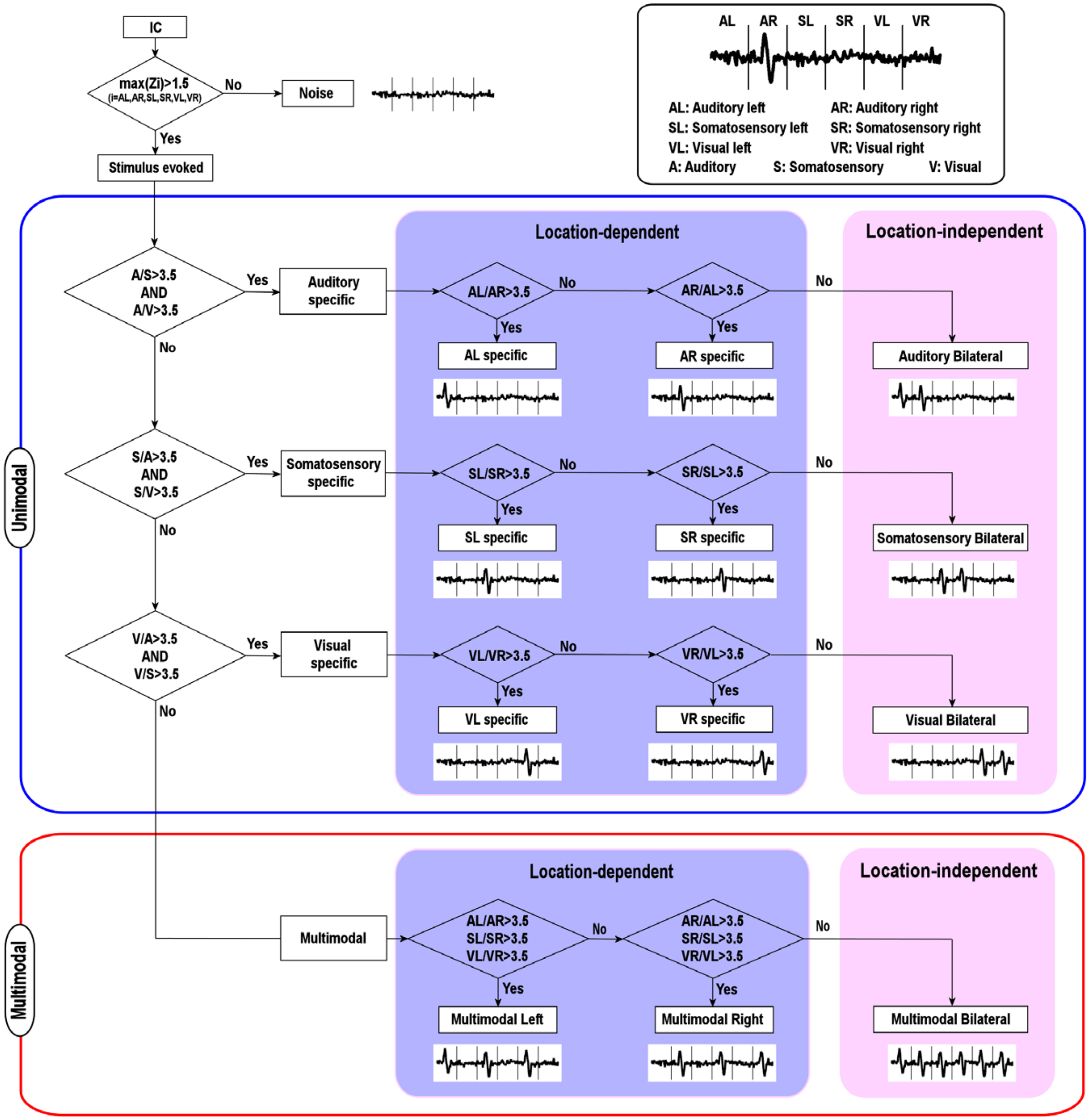

Fig. 2. Flow chart of the classification procedure of each independent component (IC). ICs were initially classified as representing noise or stimulus-evoked neural activity. Stimulus-evoked ICs were further classified as unimodal or multimodal, and then as location-dependent or location-independent, according to the ratios of Z scores between conditions. Z score of each condition is denoted as the abbreviation of the condition name (e.g. 'AL' indicates the Z score for the ERP to left auditory stimulation). An illustrative ERP time course is shown for each IC category. The inset on the top right corner shows a schematic time course for a unimodal location-dependent IC, contributing specifically to the ERP elicited by auditory stimuli presented on the right side.

the ICs as modality and location dependent. IC classification obtained using different cut-off values for defining noise-related ICs (ranging between 1.5 and 2) and modality/location-dependent ICs (ranging between 2.5 and 5) yielded results that were not significantly different from those obtained using the thresholds of 1.5 and 3.5. A comparison of the results obtained using different thresholds is reported in Supplementary Fig. S2.

2.8. Data reconstruction

In order to evaluate the contribution of each IC category to the ERP elicited by each of the six stimulus types, all the ICs belonging to a given category were recombined and back-projected on the scalp. For each participant, the contribution of each IC category to the ERPs elicited by each stimulus type was then expressed as the percentage of explained ERP variance.

3. Results

3.1. Behavioural results

All participants reported the number of stimuli presented in each block reliably, with an average error rate of 1.6 ± 2.0

(mean ± SD). The average ratings for stimulus saliency (auditory: 6.5 ± 1.8; somatosensory: 6.2 ± 1.5; visual: 6.7 ± 1.3) were not significantly different across sensory modalities ($F = 0.36$, $P = 0.7$, one-way repeated measures ANOVA).

In the control experiment performed to test the ability of participants to discriminate correctly the side of sensory stimulation, all participants determined correctly the location of all stimuli, i.e. the error rates were 0% for all participants and for all stimulus types.

3.2. ERP waveforms and topographies

Grand-average and single-subject ERP waveforms and scalp topographies are shown in Fig. 3. All ERPs consisted of a large negative-positive biphasic wave (auditory ERPs: N1-P2; somatosensory ERPs: N1-P2; visual ERPs: N1-P3), displaying a central topographical distribution, maximal at the scalp vertex. Peak latency values of the main negative and positive peaks are reported in Fig. 3. The scalp distribution of the positive peak was remarkably similar, whatever the sensory modality and the side of the stimulus. In contrast, the scalp distribution of the negative peak was noticeably different across sensory modalities. While the scalp topography of the auditory N1 extended bilaterally towards temporal regions and was symmetrically distributed over both hemispheres, the scalp topography of the somatosensory N1 extended predominantly over the hemisphere contralateral to the stimulated side, and the scalp topography of the visual N1 extended towards temporal and occipital areas.

3.3. Blind source separation of ERPs

The estimated number of independent sources contributing to the concatenated ERP waveform ranged from 12 to 20 (16.3 ± 2.8) across participants. Constraining ICA to these values preserved 99.6 ± 0.04% of the variance of all six ERP waveforms. The number of ICs in each category and the contribution of each IC category to each ERP are summarized in Table 1. 3.5 ± 3.0 ICs in each participant were classified as *Noise*. These ICs were not analysed further, as they were assumed to reflect a mixture of non-stimulus-related EEG activity and artifacts. Remaining ICs, accounting for 92.8 ± 1.3% of the variance of all six ERP waveforms, were further categorized, according to their relative contribution to the left

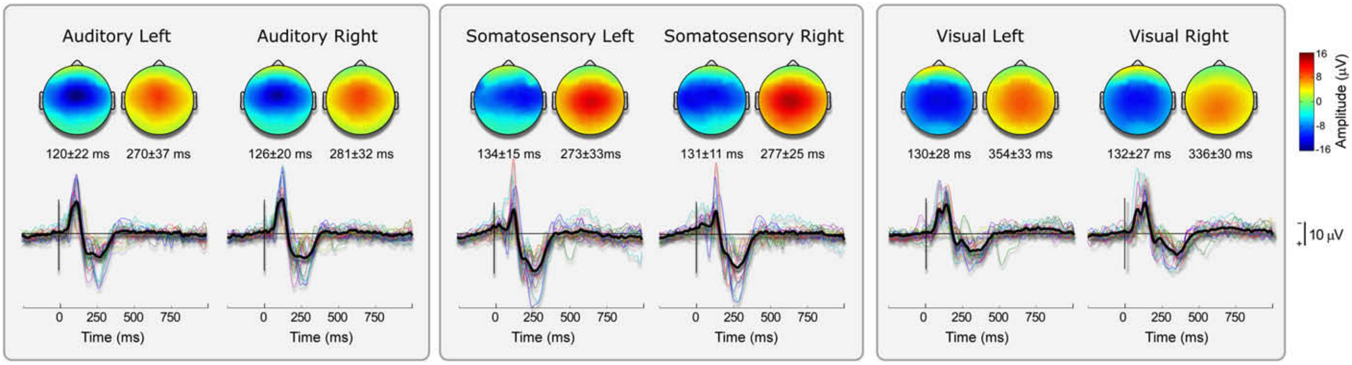

Fig. 3. ERP waveforms and scalp topographies of auditory (left panel), somatosensory (middle panel) and visual (right panel) ERPs. Displayed signals are recorded from the vertex (Cz vs. nose reference). The coloured waveforms represent single-subject ERPs, while the thick black waveform represents the grand average across subjects. Vertical lines mark the stimulus onset. Scalp topographies at the latencies of the main negative and positive peaks (mean ± SD) are shown above each ERP waveform. (For interpretation of colour mentioned in this figure legend the reader is referred to the web version of the article.)

Table 1
Number of ICs in each category, and corresponding contribution to the ERP signal.

IC category		Number of ICs (total)	Number of ICs (mean ± SD)	AL-ERP (%, mean ± SD)	AR-ERP (%, mean ± SD)	EL-ERP (%, mean ± SD)	ER-ERP (%, mean ± SD)	VL-ERP (%, mean ± SD)	VR-ERP (%, mean ± SD)
Unimodal									
Location-dependent	AL	0	0.0 ± 0.0	0.0 ± 0.0	0.0 ± 0.0	0.0 ± 0.0	0.0 ± 0.0	0.0 ± 0.0	0.0 ± 0.0
	AR	0	0.0 ± 0.0	0.0 ± 0.0	0.0 ± 0.0	0.0 ± 0.0	0.0 ± 0.0	0.0 ± 0.0	0.0 ± 0.0
	SL	10	0.8 ± 0.6	1.5 ± 1.8	1.4 ± 1.5	7.0 ± 8.0	1.5 ± 2.1	1.2 ± 1.5	1.1 ± 1.5
	SR	9	0.7 ± 0.6	0.8 ± 0.9	0.8 ± 1.0	0.8 ± 1.1	3.8 ± 4.4	0.8 ± 1.1	0.9 ± 1.3
	VL	2	0.2 ± 0.4	1.1 ± 3.2	1.4 ± 4.5	1.0 ± 3.2	0.7 ± 2.4	2.9 ± 10.0	1.1 ± 3.5
	VR	2	0.2 ± 0.4	0.8 ± 2.2	1.4 ± 4.3	0.8 ± 2.2	1.0 ± 3.0	1.9 ± 6.4	3.6 ± 10.8
Location-independent	A	9	0.7 ± 0.9	10.5 ± 16.4	13.3 ± 21.8	3.1 ± 5.5	3.7 ± 7.9	2.9 ± 6.5	2.4 ± 4.6
	S	12	0.9 ± 1.0	1.1 ± 1.6	1.1 ± 1.4	2.7 ± 4.3	2.0 ± 2.6	1.5 ± 3.0	1.0 ± 1.5
	V	25	1.9 ± 1.3	6.2 ± 6.7	8.0 ± 8.1	5.7 ± 5.0	5.5 ± 5.5	26.5 ± 22.9	30.5 ± 29.3
Multimodal									
Location-dependent	Left	1	0.1 ± 0.3	0.3 ± 1.0	0.2 ± 0.8	0.2 ± 0.8	0.1 ± 0.5	0.2 ± 0.7	0.2 ± 0.7
	Right	3	0.2 ± 0.4	0.4 ± 0.8	0.6 ± 1.6	0.4 ± 0.8	1.1 ± 2.5	0.4 ± 0.9	0.6 ± 1.2
Location-independent		94	7.2 ± 1.9	71.9 ± 34.5	72.3 ± 33.0	71.9 ± 26.0	65.1 ± 24.3	54.6 ± 35.0	49.1 ± 35.3
Summary									
Stimulus-evoked		167	12.8 ± 2.5	92.7 ± 11.7	92.9 ± 10.8	94.7 ± 8.8	90.8 ± 9.0	93.3 ± 9.7	92.2 ± 11.3
All ICs		212	16.3 ± 2.8	99.7 ± 0.2	99.6 ± 0.3	99.6 ± 0.3	99.6 ± 0.4	99.6 ± 0.5	99.6 ± 0.4

Abbreviations: A = auditory; S = somatosensory; V = visual; AL = auditory left; AR = auditory right; SL = somatosensory left; SR = somatosensory right; VL = visual left; VR = visual right.

and the right AEP, SEP and VEP segments of the concatenated ERP waveform (Fig. 2).

3.4. Multimodal Location-independent components

Multimodal Location-independent ICs (7.2 ± 1.9; Fig. 4) were the main constituent of ERPs of all three sensory modalities, explaining 71.9 ± 34.5% and 72.3 ± 33% of the left and right AEP, 71.9 ± 26% and 65.1 ± 24.3% of the left and right SEP, 54.6 ± 35% and 49.1 ± 35.3% of the left and right VEP. For all three modalities of stimulation, this *Multimodal Location-independent* activity consisted of a negative-positive biphasic wave, maximal at the vertex (Fig. 4). The scalp topography of the negative peak extended bilaterally towards temporal regions, while the scalp topography of the positive peak was more centrally distributed. The latencies of both peaks coincided with the latencies of the negative and positive peaks of the large negative-positive ERP wave (Figs. 3 and 4).

3.5. Multimodal Location-dependent components

The number of *Multimodal Location-dependent* ICs was very small. Indeed, only 0.1 ± 0.3 ICs were identified as being elicited by stimuli of all sensory modalities when presented on the left side, and only 0.2 ± 0.4 ICs were identified as being elicited by stimuli of all sensory modalities when presented on the right side.

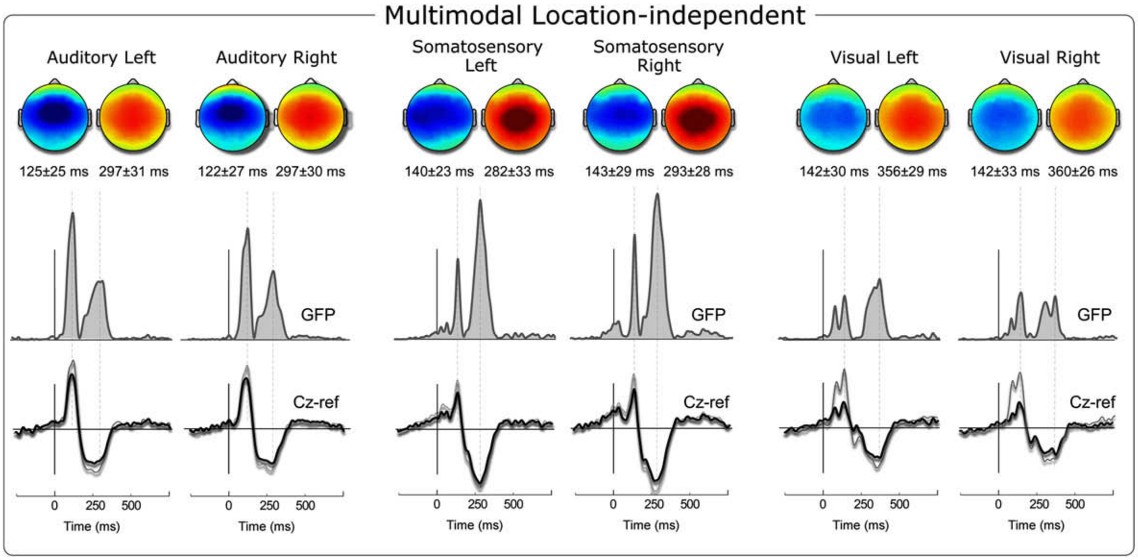

Fig. 4. *Multimodal Location-independent* components contributing to auditory, somatosensory and visual ERPs. The top row shows the scalp topographies of the two largest peaks found in the global field power time courses, displayed in the middle row. The bottom row shows the signals obtained by back-projecting the multimodal-location-independent components (thick black waveforms) onto the vertex (Cz vs. nose reference). The original ERP waveforms (grey line) are superimposed for comparison.

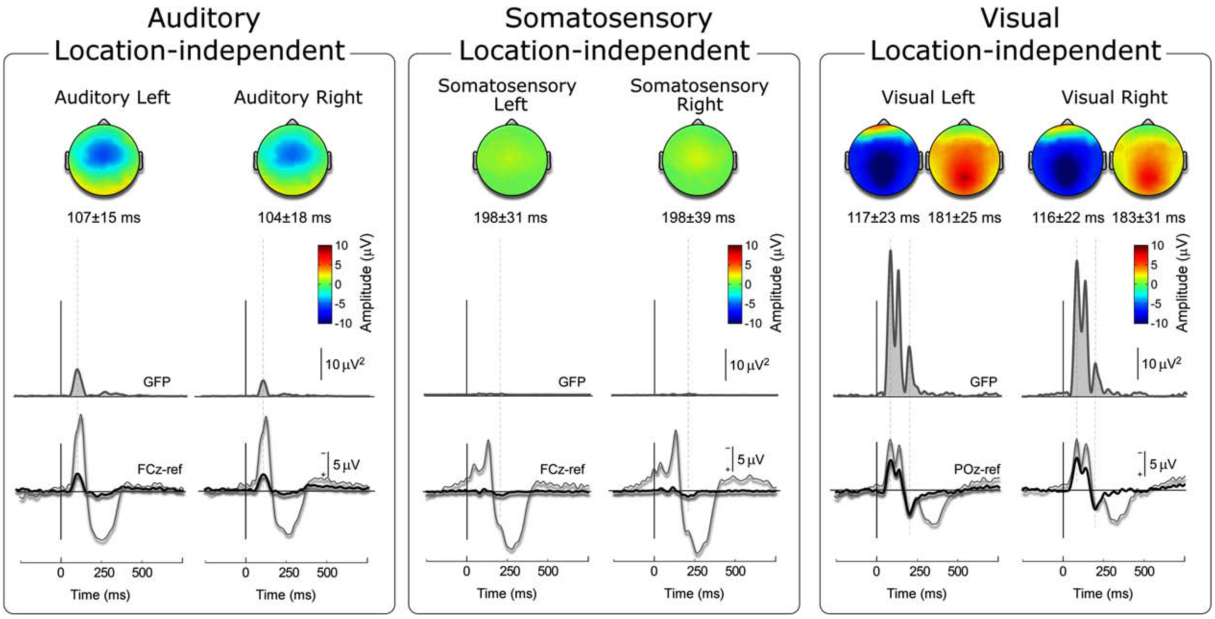

Fig. 5. *Unimodal Location-independent* components contributing to auditory, somatosensory and visual ERPs. The top row shows the scalp topographies of the peaks found in the global field power time course, displayed in the middle row. The bottom row shows the signals obtained by back-projecting *Unimodal Side-independent* components (thick black waveforms) onto the channels where the activity was maximal: FCz for the left and the right auditory and somatosensory stimulation, and POz for the left and the right visual stimulation. The original ERP waveforms (grey line) are superimposed for comparison.

Furthermore, the contribution of these *Location-dependent Multimodal* ICs to the recorded ERPs was negligible (0.5%).

3.6. Unimodal Location-independent components

Independent components representing unimodal, location-independent neural activities, were observed in all participants, and explained a fairly large portion of the recorded ERP waveforms (Fig. 5).

Auditory-specific Location-independent ICs (0.7 ± 0.9 ICs contributing to both the left and the right AEPs) explained 10.5 ± 16.4% of the variance of the AEP following left-side stimulation and 13.3 ± 21.8% of the variance of the AEP following right-side stimulation (Fig. 5 and Table 1). These ICs contributed mainly to the early part of the AEP waveform, where they formed a negative wave (peak latency: 107 ± 15 and 104 ± 18 ms for the left and the right auditory stimulation) whose scalp topography was symmetrically distributed over central, frontal, and temporal regions (Fig. 5).

Somatosensory-specific Location-independent ICs contributed minimally to the left and right SEP waveforms (0.9 ± 1.0 ICs contributing to 2.7 ± 4.3% of the variance of the SEP following left-side stimulation and 2.0 ± 2.6% of the variance of the SEP following right-side stimulation; see also Fig. 5 and Table 1).

Visual-specific Location-independent ICs (1.9 ± 1.3, contributing to both the left and right VEP) explained a large part of both the variance of the VEP following left-side stimulation (26.5 ± 22.9%) and the variance of the VEP following right-side stimulation (30.5 ± 29.3%). These ICs appeared as a large negative wave (peak latency: 117 ± 23 and 116 ± 22 ms for the left and the right visual stimulation) whose scalp topography spread over central and occipital areas, followed by a smaller positive wave (peak latency: 181 ± 25 and 183 ± 31 ms for the left and the right visual stimulation) whose scalp topography was maximal at Pz.

3.7. Unimodal Location-dependent components

Independent components representing unimodal, location-dependent neural activities, were identified in most participants ($n = 10$), and explained a relatively small portion of the recorded ERP waveforms (Fig. 6).

Across all participants, not a single *Auditory-specific Location-dependent* IC was identified.

In contrast, *Somatosensory-specific Location-dependent* ICs were identified in most participants (0.8 ± 0.6 ICs contributing specifically to the SEP following left-side stimulation, 0.7 ± 0.6 ICs contributing specifically to the SEP following right-side stimulation). These ICs explained 7.0 ± 8.0% and 3.8 ± 4.4% of the variance of the left and the right SEPs, and appeared as a negative wave (peak latency: 100 ± 25 and 95 ± 23 ms for the left and the right somatosensory stimulation) whose scalp topography was clearly maximal over the hemisphere contralateral to the stimulated side (FCC4H and FCC3H for the left and the right somatosensory stimulation; Fig. 6).

Visual-specific Location-dependent ICs (0.2 ± 0.4 ICs contributing specifically to the VEP following left-side stimulation and 0.2 ± 0.4 ICs contributing specifically to the VEP following right-side stimulation) explained only 2.9 ± 10% and 3.6 ± 10.8% of the variance of the left and the right VEPs. These ICs formed a negative wave (peak latency: 151 ± 4 and 175 ± 32 ms for the left and the right visual stimulation), and displayed a contralateral posterior distribution, maximal over occipital areas (P6 and P5 for the left and the right visual stimulation; Fig. 6).

4. Discussion

Using P-ICA, we were able to separate the ERPs elicited by stimuli belonging to different sensory modalities (auditory, somatosensory and visual) into a set of *Unimodal* and *Multimodal* components, thus confirming the results of our previous study (Mouraux and Iannetti, 2009). Furthermore, by delivering sensory stimuli to two distinct spatial locations (left and right sides), we were able to further classify *Unimodal* and *Multimodal* components as *Location-dependent* and *Location-independent*. Our results may be summarized as follows. (1) Middle-latency sensory ERPs can be explained by a large contribution of *Multimodal* neural activities, and a

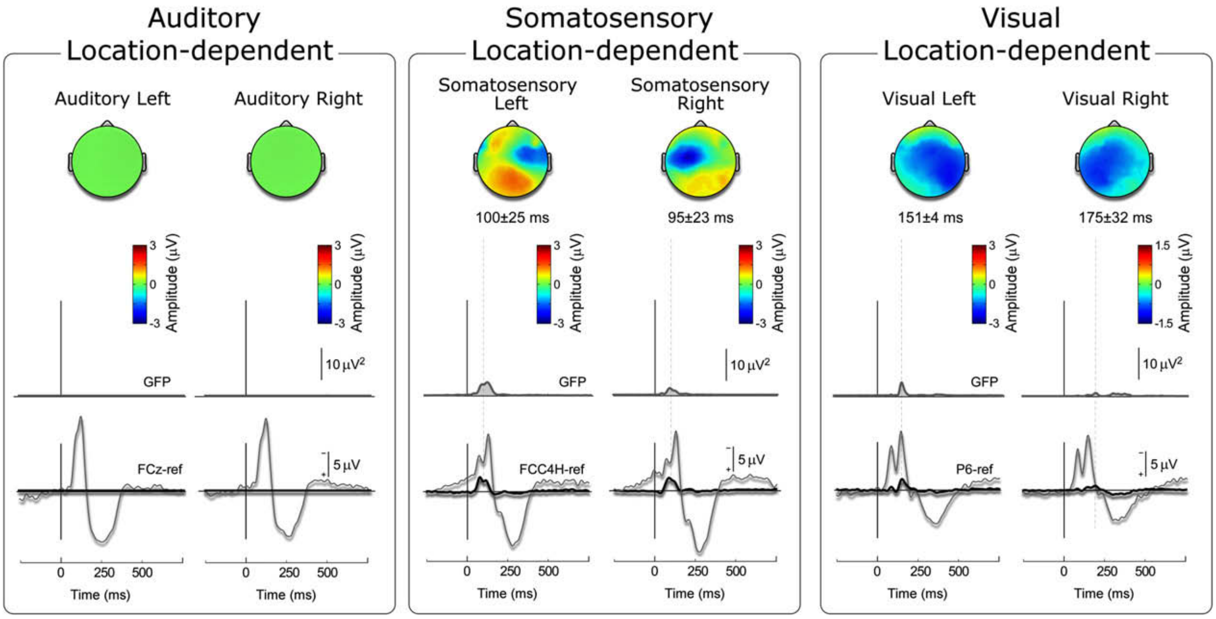

Fig. 6. *Unimodal Location-dependent* components contributing to auditory, somatosensory and visual ERPs. The top row shows the scalp topographies of the peaks found in the global field power time course, displayed in the middle row. The bottom row shows the signals obtained by back-projecting *Unimodal Side-dependent* components (thick black waveforms) onto the channel where the activity was maximal: FCC4H and FCC3H for the left and the right somatosensory stimulation, respectively, P6 and P5 for the left and the right visual stimulation, respectively. Note, there is no *Auditory Side-dependent* ICs. The original ERP waveforms (grey line) are superimposed for comparison.

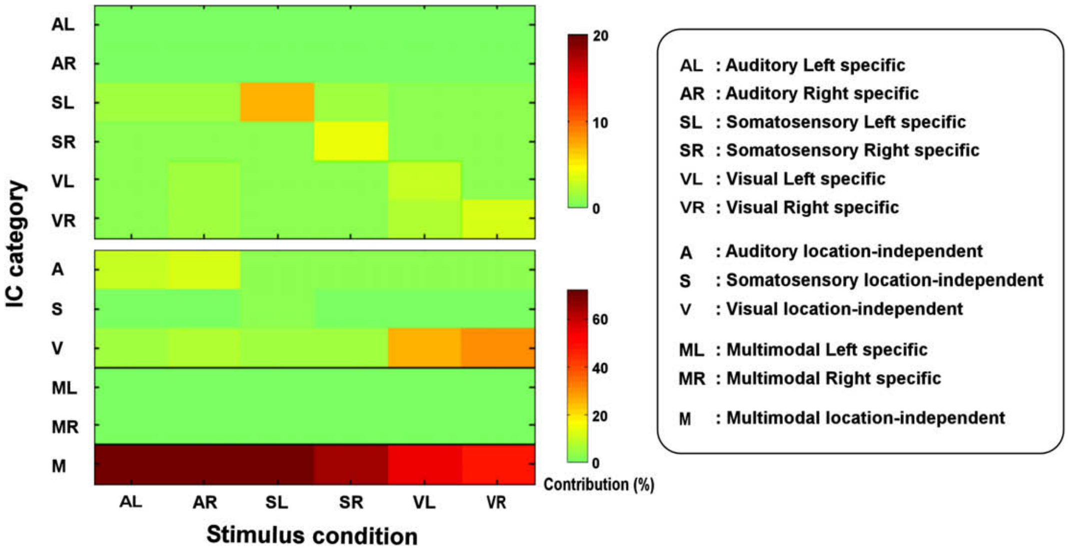

Fig. 7. Contribution of each IC category to the sensory ERPs. The contribution is colour-coded, and defined as percentage of the ERP variance explained by each IC category. Rows in the matrix represent IC categories and columns represent sensory ERPs. Note how sensory ERPs are explained by a predominant contribution of multimodal neural activities (bottom row), and a smaller contribution of unimodal neural activities (upper rows).

smaller contribution of *Unimodal* neural activities. (2) *Multimodal* neural activities are mainly *Location-independent*, as the contribution of *Location-dependent* components is negligible. (3) A fraction of *Unimodal* neural activities is *Location-dependent*, especially when considering the ERP elicited by somatosensory stimuli. (4) A fraction of *Unimodal* neural activities is *Location-independent*, especially when considering the ERPs elicited by auditory and visual stimuli.

4.1. Multimodal components

Consistent with our previous findings, *Multimodal* neural activities represent the main constituent of middle-latency scalp ERPs (Figs. 4 and 7). As a rather long inter-stimulus interval was used, it is likely that the contribution of these *Multimodal* neural activities was maximised because of the attentional reorientation triggered by infrequent stimuli. Indeed, in a previous study (Mouraux and Iannetti, 2009), we observed a significant correlation between the magnitude of these multimodal neural activities and the subjective rating of stimulus saliency, thus suggesting that these activities are involved in stimulus-triggered mechanisms of arousal or attentional reorientation[5]. By comparing the responses elicited by stimuli applied to the left and right hemibodies, we were able to examine whether some of these *Multimodal* neural activities were dependent on the location of the eliciting stimulus. Although there is fMRI and single-cell electrophysiological evidence suggesting the existence of *Multimodal Location-dependent* cortical activities (Graziano and Gross, 1995; Macaluso and Driver, 2001), our results indicate that these neural activities cannot be isolated in scalp ERP recordings. Indeed, the contribution of *Multimodal* ICs classified as *Location-dependent* was negligible: *Multimodal* left location-dependent ICs explained only 0.2% of the variance of left ERPs, and *Multimodal Right Location-dependent* ICs explained only 0.8% of the variance of right ERPs.

Several explanations for the inability to isolate *Multimodal Location-dependent* components in scalp ERPs can be put forward.

First, the electric field generated by these components may be too weak or organized in such a way that it does not translate into a measurable scalp EEG signal (e.g. closed fields; Nunez and Srinivasan, 2006). In support of this explanation, *Location-dependent Multimodal* responses have been recorded from deep subcortical structures (e.g. the putamen; Graziano and Gross, 1995), which are unlikely to generate activity translating into a measurable scalp potential, both because of their distance from the scalp and because of their spatial configuration (Nunez and Srinivasan, 2006).

Second, *Multimodal Location-dependent* neural activities may contribute to the scalp ERP response, but the scalp topography of the response elicited by left- and right-side stimulation may be either too similar to each other, or too similar to the scalp topography of *Location-independent* neural activities to be separated effectively using P-ICA. This would occur if the activated neuronal populations are intermingled or closely located. In support of this explanation, it has been shown that the peak of the location-dependent BOLD-fMRI response to contralateral visual and tactile stimulation, located in the anterior part of the intraparietal sulcus, was adjacent to the peak of the location-independent response to the same stimuli (Macaluso and Driver, 2001). Furthermore, single-cell recordings in macaque monkeys have shown that location-dependent multimodal neurons can be intermingled with location-independent multimodal neurons, for example, in the putamen and inferior premotor cortex (Graziano and Gross, 1995).

4.2. Unimodal components

Besides the predominant contribution of *Multimodal* components to middle-latency scalp ERPs, we were able to isolate a number of *Unimodal* components (Figs. 5 and 6). Unlike *Multimodal* components, a significant fraction of these *Unimodal* components were dependent on the spatial location of the sensory stimulus (Fig. 7).

Somatosensory-specific components were clearly separated into a set of *Location-dependent* and *Location-independent* neural activities. *Location-dependent* ICs (explaining approximately 5% of the SEP waveform) were predominant as compared to *Location-independent* ICs (explaining approximately 2% of the SEP waveform).

---

[5] Such an interpretation can also explain the relatively large inter-individual differences in the relative contribution of multimodal components, which could thus reflect variations in vigilance or attentional focus across participants.

The predominance of *Somatosensory-specific Location-dependent* components is consistent with the known anatomical pathway for the transmission of vibrotactile somatic information: large-fibre primary afferent neurons enter the spinal cord and ascend ipsilaterally, second-order neurons decussate in the brain stem, ascend to the thalamus and third-order thalamocortical neurons terminate in the primary somatosensory cortex located in the postcentral gyrus contralateral to the side of stimulation (Gardner et al., 2000). However, neural responses to somatosensory stimuli are not strictly restricted to contralateral stimulation. Electrophysiological studies in monkeys have shown that in the upper bank of the intra-parietal sulcus (Iwamura et al., 1994), in the secondary somatosensory cortex (Robinson and Burton, 1980) and in Brodmann's areas 5 and 7 in the parietal cortex (Burbaud et al., 1991; Duffy and Burchfiel, 1971; Mountcastle et al., 1975; Sakata et al., 1973), some neurons have bilateral receptive fields. This finding, combined with the fact that these regions have dense callosal connections, suggests that these neurons may be involved in the transfer of tactile information between hemispheres. This would agree with the notion that these cortical areas support complex somatosensory functions, such as the integration of sensory information that is necessary for co-operative actions of the two hands (Duffy and Burchfiel, 1971; Iwamura et al., 1994; Manzoni et al., 1989). Therefore, *somatosensory-specific Location-independent* neural activities would reflect late stages of somatosensory processing, underlying more complex processing based on the binding of different features of the stimuli to gain a coherent percept (Mountcastle, 2005). Consistent with this notion, *Somatosensory-specific Location-independent* components tended to peak later than *Somatosensory-specific Location-dependent* components (Figs. 5 and 6).

Similarly, *Visual-specific* components were clearly separated into a set of *Location-dependent* and *Location-independent* neural activities. However, in contrast with the *Somatosensory-specific* components, *Location-independent Visual-specific* ICs (explaining approximately 29% of the VEP waveform) were predominant as compared to *Location-dependent Visual-specific* ICs (explaining approximately 3% of the VEP waveform). The visual information collected by the nasal hemiretina is transmitted through axons of the optic nerve that, at the optic chiasm, cross the midline and project to the contralateral lateral geniculate nucleus. In contrast, the visual information collected by the temporal hemiretina is transmitted through axons of the optic nerve that do not cross the midline and project to the ipsilateral lateral geniculate nucleus. Therefore, each hemisphere receives a complete representation of the contralateral visual hemifield. This anatomical organisation of the visual system supports the finding of *Visual-specific Location-dependent* components. However, the neural circuitry of the visual system involves extensive bilateral connections between the two hemispheres (Wurtz and Kandel, 2000), related to the construction of a unitary visual percept, uniting the left and right visual hemifields. Indeed, ipsilateral responses to visual stimuli have been described in extrastriate visual cortical areas using fMRI (Tootell et al., 1998). The important role played by this bilateral visual processing (Clarke and Zaidel, 1989; Marsolek et al., 2002; Myers and Sperry, 1985) could explain the large contribution of *Visual-specific Location-independent* components. In agreement with this hypothesis, VEP components independent of stimulus location have been described (Nalcaci et al., 1999; Srebro, 1985, 1987). In particular, while the early (∼90 ms) components of VEPs elicited by pattern pulse stimuli are sensitive to the spatial location of the stimulus, later (∼130 ms) components are less sensitive to stimulus location, and can be elicited by stimuli presented both in the ipsilateral and contralateral visual hemifield (Srebro, 1987). One obvious explanation for the observation of such large *Visual-specific Location-independent* neural activities would be inter-hemispheric connections between symmetric cortical areas through the corpus callosum (Berardi et al., 1989; Wurtz and Kandel, 2000). Alternatively, the spatial proximity between left and right visual areas could also explain, at least in part, the large contribution of *Visual-specific Location-independent* components to visual ERPs. Indeed, while the hand areas in the left and right somatosensory cortices are well separated in space, the left and right visual areas are closer to each other, and the scalp distribution of their projected activity might be similar. Therefore, we must consider the possibility that P-ICA was unable to separate a fraction of left and right *Location-dependent Visual-specific* components, which, for that reason, might have been classified as *Location-independent*.

Finally, *Auditory-specific* components contributed significantly to both the left and the right auditory ERP. In contrast with *Somatosensory-* and *Visual-specific* components, and similarly to *Multimodal* components, not a single *Auditory-specific* IC was dependent on the side of stimulation, thus indicating that the scalp distributions of AEPs elicited by left- and right-side stimuli in our experiment were spatially indistinguishable. This observation is consistent with the notion that the processing of auditory input is not as lateralized as the processing of visual and somatosensory input. Indeed, while the topographic arrangements of neurons in primary somatosensory and visual cortices reflects the location of a somatosensory stimulus on the body or of a visual stimulus in the external world, the topographic arrangements of neurons in primary auditory cortex reflects the frequency of a sound, but not its location in space. Furthermore, extensive binaural interactions occur already in the auditory structures of the brainstem, which rely on minimal interaural time and intensity cue differences to localise sounds in space. Consequently, the ascending cortical projections are largely binaural, and the primary auditory cortex in each hemisphere is largely responsive to stimuli presented to both the left and the right ear. In addition, our stimuli were not monoaural, but delivered from lateralised sources located close to the left or the right hand, and were thus activating both the left and the right cochlear receptors. Although both time and intensity differences between right-ear and left-ear sensory inputs are crucial to localize auditory stimuli in space, the unavoidable use of binaural stimulation might have biased our results towards a greater contribution of *Location-independent* components than of *Location-dependent* components. However, the feature of less lateralization in auditory cortex has led to contradictory findings by previous neuroimaging studies on the lateralisation of the cortical responses to auditory stimulation, even when strict monaural stimulation is considered: a number of studies have reported greater responses in the hemisphere contralateral to the stimulated ear (Ackermann et al., 2001; Hine and Debener, 2007; Picton et al., 1999), while other studies were unable to confirm the existence of such a lateralization (Devlin et al., 2003; Goff et al., 1977; Schonwiesner et al., 2007).

In conclusion, this study shows that P-ICA is an effective tool to break down ERPs into spatially-distinct and temporally-independent neural activities. Here we used P-ICA to decompose ERPs elicited by stimuli of different sensory modalities into *Unimodal* and *Multimodal* components, and to further break them down into *Location-dependent* and *Location-independent* components, according to whether or not they are sensitive to the spatial location of the eliciting stimulus. By doing this we provided a quantitative analysis of the relative contribution of each constituent to the recorded signal, thus understanding better the functional significance of sensory ERPs. Furthermore, this approach has the potential to identify the effect of experimental manipulations on the different neural activities reflected by scalp ERPs. For example, in studies on multisensory integrations, P-ICA would be helpful to isolate and provide a quantitative measure of the neural activities specifically underlying multisensory integration from those specifically devoted to unimodal or multimodal processing.

Acknowledgments

M. Liang is supported by a grant from the Volkswagenstiftung to C. Blakemore, P. Stoerig and P. Haggort. A Mouraux is funded by the Belgian National Fund for Scientific Research. G.D. Iannetti is University Research Fellow of The Royal Society and acknowledges the support of the BBSRC. All authors are grateful to the members of the GAMFI Project for insightful comments.

Appendix A. Supplementary data

Supplementary data associated with this article can be found, in the online version, at doi:10.1016/j.clinph.2009.12.012.

References

Ackermann H, Hertrich I, Mathiak K, Lutzenberger W. Contralaterality of cortical auditory processing at the level of the M50/M100 complex and the mismatch field: a whole-head magnetoencephalography study. Neuroreport 2001;12(8): 1683–7.

Avillac M, Ben Hamed S, Duhamel JR. Multisensory integration in the ventral intraparietal area of the macaque monkey. J Neurosci 2007;27(8):1922–32.

Beckmann CF, Smith SM. Probabilistic independent component analysis for functional magnetic resonance imaging. IEEE Trans Med Imaging 2004;23(2): 137–52.

Bell AJ, Sejnowski TJ. An information-maximization approach to blind separation and blind deconvolution. Neural Comput 1995;7(6):1129–59.

Berardi N, Bodis-Wollner I, Fiorentini A, Giuffre G, Morelli M. Electrophysiological evidence for interhemispheric transmission of visual information in man. J Physiol 1989;411:207–25.

Burbaud P, Doegle C, Gross C, Bioulac B. A quantitative study of neuronal discharge in areas 5, 2, and 4 of the monkey during fast arm movements. J Neurophysiol 1991;66(2):429–43.

Clarke JM, Zaidel E. Simple reaction times to lateralized light flashes. Varieties of interhemispheric communication routes. Brain 1989;112(Pt. 4):849–70.

Delorme A, Makeig S. EEGLAB: an open source toolbox for analysis of single-trial EEG dynamics including independent component analysis. J Neurosci Methods 2004;134(1):9–21.

Devlin JT, Raley J, Tunbridge E, Lanary K, Floyer-Lea A, Narain C, et al. Functional asymmetry for auditory processing in human primary auditory cortex. J Neurosci 2003;23(37):11516–22.

Duffy FH, Burchfiel JL. Somatosensory system: organizational hierarchy from single units in monkey area 5. Science (New York, NY. 1971;172(980):273–5.

Duhamel JR, Colby CL, Goldberg ME. Ventral intraparietal area of the macaque: congruent visual and somatic response properties. J Neurophysiol 1998;79(1):126–36.

Fogassi L, Gallese V, Fadiga L, Luppino G, Matelli M, Rizzolatti G. Coding of peripersonal space in inferior premotor cortex (area F4). J Neurophysiol 1996;76(1):141–57.

Garcia-Larrea L, Lukaszewicz AC, Mauguiere F. Somatosensory responses during selective spatial attention: the N120-to-N140 transition. Psychophysiology 1995;32(6):526–37.

Gardner EP, Martin JH, Jessell TM. The bodily senses. In: Kandel ER, Schwartz JH, Jessell TM, editors. Princeples of neural science. Elsevier Science; 2000. p. 430–50.

Goff GD, Matsumiya Y, Allison T, Goff WR. The scalp topography of human somatosensory and auditory evoked potentials. Electroencephalogr Clin Neurophysiol 1977;42(1):57–76.

Graziano MS. Where is my arm? The relative role of vision and proprioception in the neuronal representation of limb position. Proc Natl Acad Sci USA 1999;96(18):10418–21.

Graziano MS, Cooke DF, Taylor CS. Coding the location of the arm by sight. Science (New York, NY) 2000;290(5497):1782–6.

Graziano MS, Gross CG. A bimodal map of space: somatosensory receptive fields in the macaque putamen with corresponding visual receptive fields. Exp Brain Res Experimentelle Hirnforschung 1993;97(1):96–109.

Graziano MS, Gross CG. The representation of extrapersonal space: a possible role for bimodal visual-tactile neurons. In: Gazzaniga MS, editor. The cognitive neurosciences. Cambridge: MIT press; 1995. p. 1021–1034.

Hine J, Debener S. Late auditory evoked potentials asymmetry revisited. Clin Neurophysiol 2007;118(6):1274–85.

Iannetti GD, Niazy RK, Wise RG, Jezzard P, Brooks JC, Zambreanu L, et al. Simultaneous recording of laser-evoked brain potentials and continuous, high-field functional magnetic resonance imaging in humans. NeuroImage 2005;28(3):708–19.

Ikeda H, Nishijo H, Miyamoto K, Tamura R, Endo S, Ono T. Generators of visual evoked potentials investigated by dipole tracing in the human occipital cortex. Neuroscience 1998;84(3):723–39.

Iwamura Y, Iriki A, Tanaka M. Bilateral hand representation in the postcentral somatosensory cortex. Nature 1994;369(6481):554–6.

Jung TP, Makeig S, Humphries C, Lee TW, McKeown MJ, Iragui V, et al. Removing electroencephalographic artifacts by blind source separation. Psychophysiology 2000;37(2):163–78.

Jutai JW, Gruzelier JH, Connolly JF. Spectral analysis of the visual evoked potential (VEP): effects of stimulus luminance. Psychophysiology 1984;21(6):665–72.

Kayser C, Petkov CI, Lippert M, Logothetis NK. Mechanisms for allocating auditory attention: an auditory saliency map. Curr Biol 2005;15:1943–7.

Legrain V, Guerit JM, Bruyer R, Plaghki L. Attentional modulation of the nociceptive processing into the human brain: selective spatial attention, probability of stimulus occurrence, and target detection effects on laser evoked potentials. Pain 2002;99:21–39.

Luck SJ. An introduction to the event-related potential technique. Cambridge: The MIT Press; 2005.

Macaluso E, Driver J. Spatial attention and crossmodal interactions between vision and touch. Neuropsychologia 2001;39(12):1304–16.

Makeig S, Jung TP, Bell AJ, Ghahremani D, Sejnowski TJ. Blind separation of auditory event-related brain responses into independent components. Proc Natl Acad Sci USA 1997;94(20):10979–84.

Manzoni T, Barbaresi P, Conti F, Fabri M. The callosal connections of the primary somatosensory cortex and the neural bases of midline fusion. Exp Brain Res Experimentelle Hirnforschung. 1989;76(2):251–66.

Maravita A, Spence C, Driver J. Multisensory integration and the body schema: close to hand and within reach. Curr Biol 2003;13(13):R531–9.

Marsolek CJ, Nicholas CD, Andresen DR. Interhemispheric communication of abstract and specific visual-form information. Neuropsychologia 2002;40(12): 1983–99.

Mountcastle VB. The sensory hand: neural mechanisms of somatic sensation. Harvard University Press; 2005.

Mountcastle VR, Lynch JC, Georgopoulos A, Sakata H, Acuna C. Posterior parietal association cortex of the monkey: command functions for operations within extrapersonal space. J Neurophysiol 1975;38:871–908.

Mouraux A, Iannetti GD. Across-trial averaging of event-related EEG responses and beyond. Magn Reson Imaging 2008;26:1041–54.

Mouraux A, Iannetti GD. Nociceptive laser-evoked brain potentials do not reflect nociceptive-specific neural activity. J Neurophysiol 2009;101(6):3258–69.

Myers JJ, Sperry RW. Interhemispheric communication after section of the forebrain commissures. Cortex 1985;21(2):249–60.

Naatanen R, Picton T. The N1 wave of the human electric and magnetic response to sound: a review and an analysis of the component structure. Psychophysiology 1987;24(4):375–425.

Nalcaci E, Basar-Eroglu C, Stadler M. Visual evoked potential interhemispheric transfer time in different frequency bands. Clin Neurophysiol 1999;110(1):71–81.

Nunez PL, Srinivasan R. Electric fields of the brain. The neurophysics of EEG. New York: Oxford University Press; 2006.

Picton TW, Alain C, Woods DL, John MS, Scherg M, Valdes-Sosa P, et al. Intracerebral sources of human auditory-evoked potentials. Audiol Neurootol 1999;4(2): 64–79.

Rajan JJ, Rayner PJW. Model order selection for the singular value decomposition and the discrete Karhunen–Loeve transform using a Bayesian approach. Vis Image Signal Process IEEE Proc 1997;144:116–23.

Regan D. Human brain electrophysiology: evoked potentials and evoked magnetic fields in science and medicine. New York: Elsevier; 1989.

Robinson CJ, Burton H. Somatotopographic organization in the second somatosensory area of M. fascicularis. J Comp Neurol 1980;192(1):43–67.

Sakata H, Takaoka Y, Kawarasaki A, Shibutani H. Somatosensory properties of neurons in the superior parietal cortex (area 5) of the rhesus monkey. Brain Res 1973;64:85–102.

Schlereth T, Baumgartner U, Magerl W, Stoeter P, Treede RD. Left-hemisphere dominance in early nociceptive processing in the human parasylvian cortex. NeuroImage 2003;20:441–54.

Schonwiesner M, Krumbholz K, Rubsamen R, Fink GR, von Cramon DY. Hemispheric asymmetry for auditory processing in the human auditory brain stem, thalamus, and cortex. Cereb Cortex 2007;17(2):492–9.

Srebro R. Localization of visually evoked cortical activity in humans. J Physiol 1985;360:233–46.

Srebro R. The topography of scalp potentials evoked by pattern pulse stimuli. Vis Res 1987;27(6):901–14.

Tootell RB, Mendola JD, Hadjikhani NK, Liu AK, Dale AM. The representation of the ipsilateral visual field in human cerebral cortex. Proc Natl Acad Sci USA 1998;95(3):818–24.

Treede RD, Kief S, Holzer T, Bromm B. Late somatosensory evoked cerebral potentials in response to cutaneous heat stimuli. Electroencephalogr Clin Neurophysiol 1988;70(5):429–41.

Treede RD, Kunde V. Middle-latency somatosensory evoked potentials after stimulation of the radial and median nerves: component structure and scalp topography. J Clin Neurophysiol 1995;12(3):291–301.

Wurtz RH, Kandel ER. Central visual pathways. In: Kandel ER, Schwartz JH, Jessell TM, editors. Principles of neural science. Elseiver Science; 2000. p. 523–47.